Th-AM-Sym I-1

STRUCTURE OF AN UNUSUALLY STABLE RNA HAIRPIN, Gabriele Varani, Chaejoon Cheong & Ignacio Tinoco, Jr., Department of Chemistry and Laboratory of Chemical Biodynamics, University of California, Berkeley CA 94720.

The hairpin loop is the predominant element of RNA secondary structure. It is formed when a polynucleotide chain folds back on itself to form a base-paired helix (the stem), leaving several nucleotides unpaired (the loop). Both the size and the sequence of hairpin loops in naturally occurring RNA molecules are evolutionarily conserved. In ribosomal RNA's, most hairpin loops contain four unpaired nucleotides; although 256 different tetraloops are possible, 70% of all tetraloops in ribosomal RNA are either UNCG or GNRA (N is any nucleotide, R is a purine), and the helix is almost invariably closed by a C·G base-pair. The structure of a hairpin loop containing the very common sequence C(UUCG)G has been determined in solution by NMR spectroscopy and distance geometry (Cheong et al., 1990). Hairpins with that loop sequence show unusually high thermal stability, which decreases considerably when the conserved cytosine in the loop is mutated to uracil. The NMR data reveal the formation of a mismatched G·U base pair, with *syn* guanosine, extensive stacking of the loop nucleotides, and specific base-phosphate interactions. The formation of the G·U base pair leaves a loop of only two nucleotides. Both adopt C_2'-*endo* sugar pucker, thereby extending the phosphodiester backbone at little free energy cost. We expect this to be a general property of RNA hairpins with small loops. A sharp turn in the phosphodiester backbone is necessary to reverse the polynucleotide chain direction; the turn is stabilized by a cytosine-phosphate hydrogen bond, and by stacking of the cytosine nucleotide on the G·U base pair. These structural features can explain the unusual thermodynamic stability of this hairpin, and its sensitivity to mutations of loop nucleotides. Its compact structure and unusual stability could explain why reverse transcriptase cannot read through the loop, and suggest its role as nucleation site for RNA folding.

Cheong, C., Varani, G. & Tinoco, I. Jr. (1990) *Nature* 346, 680-682.

Th-AM-Sym I-2

Juli Feigon, Vladimír Sklenář, Román Macaya, Edmond Wang, & Dara Gilbert

Structures and Sequence Specificity of Intramolecular DNA Triplexes

Homopurine:homopyrimidine DNA sequences readily form triple stranded structures under appropriate conditions. Such sequences are over represented in the eukaryotic genome and may play a role in genetic regulation and recombination. It has been proposed that these sequences can form a structure termed H-DNA, in which a mirror repeat sequence folds back on itself to form a three-stranded structure and a single (usually purine) strand. We have been studying the conformation of intramolecular triplexes formed from folding of a single 28-31 base DNA strand, using two-dimensional NMR methods. These molecules are an excellent model system for the structure of the triple strand part of H-DNA. Information on the structure of these intramolecular triplexes will be presented. In addition to their interest because of possible roles *in vivo*, DNA triplexes are important because of their potential use as therapeutic agents, through targeting of a modified DNA oligonucleotide to a specific control sequence. An understanding of the sequence requirements and stabilities of triplexes is essential for such applications. We have substituted various base triplets into our intramolecular triplexes. Information on the formation, stability, and base pairing schemes of these alternative base triplets in the substituted intramolecular triplexes will be presented.

Th-AM-Sym I-3

THE THERMODYNAMICS OF NOVEL DNA STRUCTURES: TRIPLEXES, TETRAPLEXES, AND DUPLEXES WITH MUTAGENIC LESIONS. Kenneth J. Breslauer, Department of Chemistry, Rutgers, The State University of New Jersey, New Brunswick, NJ 08903.

We have used a combination of spectroscopic and calorimetric techniques to characterize thermodynamically the stability and melting behaviors of nucleic acid complexes which exhibit molecularities greater than 2 and of nucleic acid duplexes which contain mutagenic lesions. Specifically, we have determined the thermodynamic changes accompanying the thermally-induced disruption of a DNA triplex, an apparent DNA tetraplex, and an oligomeric DNA duplex with an abasic site. These data will be presented and discussed in terms of structural models that have been proposed for each of these DNA complexes. This work was supported by NIH Grants GM23509, GM34469,and CA47795.

Th-AM-Sym-I-4

SEQUENCE SPECIFIC RECOGNITION OF DOUBLE HELICAL DNA BY OLIGONUCLEOTIDE-DIRECTED TRIPLE HELIX FORMATION

Peter B. Dervan
Division of Chemistry and Chemical Engineering
California Institute of Technology
Pasadena, California 91125 USA

Pyrimidine oligonucleotides recognize purine sequences in the major groove of double helical DNA via triple helix formation. Specificity is imparted by Hoogsteen base pairing between the pyrimidine oligonucleotide and the purine strand of the Watson-Crick duplex DNA (TAT and C+GC base triplets). Due to the length of the recognition site (>15 base pairs), in a formal sense, this is 10^6 times more sequence specific than restriction enzymes and affords 32,268 new sequence specificities (from 2^{15}). The triple helix motif may be useful for single site cleavage of genomic DNA and the manipulation of sequence specific protein:DNA binding. With regard to molecular recognition of duplex DNA by oligonucleotides, efforts to extend the triple helix motif to all four base pairs will be discussed.

Th-AM-A1

INTERACTION OF PERMEANT AND BLOCKING IONS IN THE PORE OF DIHYDROPYRIDINE-SENSITIVE CALCIUM CHANNELS.

B.D. Winegar and J.B. Lansman.
Department of Pharmacology, School of Medicine, University of California, San Francisco, CA 94143-0450.

We investigated the effects of permeant ion concentration on the voltage dependence of blocker exit from the pore. Block by La^{3+} and Cd^{2+} of unitary calcium channel currents was recorded from cell-attached patches on the surface of C2 myotubes with 25 - 110 mM $BaCl_2$ and a fixed concentration of blocker in the patch pipette. The kinetics of block were studied by analyzing the lifetimes of discrete blocking events. The exit rate (t_C^{-1}) for La^{3+} was ~100 s^{-1} and increased to ~300 s^{-1} in the presence of 25 and 110 mM Ba^{2+}, respectively, at 0 mV. The exit rate increased ~e-fold per 22 mV and ~e-fold per 20 mV in the presence of 25 and 110 mM Ba^{2+}, respectively. The exit rate for Cd^{2+} was ~600 s^{-1} and ~2,500 s^{-1} in the presence of 25 and 110 mM Ba^{2+}, respectively. The exit of Cd^{2+} from the pore increased ~e-fold per 17 mV and ~e-fold per 21 mV in the presence of 25 and 110 mM Ba^{2+}, respectively. Thus raising $[Ba^{2+}]_o$ increases the absolute exit rate to a greater extent for Cd^{2+} than for La^{3+} (four and three-fold, respectively). $[Ba^{2+}]_o$ had little effect on the voltage-dependence of the exit rate, suggesting the applied membrane field does not clear blocker from the pore by a mechanism in which permeant ion flux drives the exit of the blocking ion.

Th-AM-A2

INACTIVATING & NON-INACTIVATING DIHYDROPYRIDINE-SENSITIVE CALCIUM CHANNELS IN CEREBELLAR NEURONS.

Jeffry B. Lansman & Paul A. Slesinger, Dept. of Pharmacology, School of Medicine, University of California, San Francisco, CA

Recordings of single-channel activity from cerebellar granule cells with 90 mM Ba in the patch electrode show the existence of a single type of channel with a conductance of ~22 pS (*Biophys. J.* 57:524a, 1990). Channel activity appears as short bursts in the beginning of a voltage pulse or as long bursts that continue throughout the pulse in either the absence or presence of the DHP agonist +202-791. A similar gating pattern is observed when monovalent cations carry charge though the channel. We conclude that non-inactivating and inactivating channel activity can arise from a single type of channel. To explain the observation that shifting the holding potential to more positive levels abolishes the decaying component of whole-cell current, we propose that channels enter a long-lived open state after inactivating. Depolarized holding potentials suppress inactivating and non-inactivating channels equally: the sum of a small inactivating component and the long openings favored by positive holding potentials produces a sustained current. We also speculate that dihydropyridines can reduce or increase total current simply by altering the equilibrium distribution of inactivated and open channels.

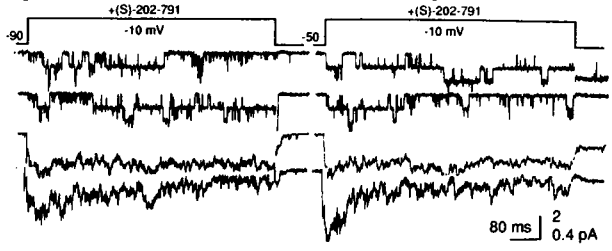

Th-AM-A3

REOPENING OF CALCIUM CHANNELS AT NEGATIVE MEMBRANE POTENTIALS DEPENDS ON CHANNEL INACTIVATION.

Paul A. Slesinger & Jeffry B. Lansman,
Department of Pharmacology, School of Medicine, University of California, San Francisco, CA 94143

Ca^{2+} channels reopen at negative membrane potentials following brief depolarizations to positive potentials (*Soc. Neurosci. Abs*: 486.1, 1990). The opening of Ca^{2+} channels at negative membrane potentials, where the driving force for Ca^{2+} entry is large, may be the physiologically relevant pathway for Ca^{2+} influx into neurons. We investigated the mechanism underlying reopening by recording from cell-attached patches on the soma of cerebellar neurons grown *in vitro* with 90 mM Ba^{2+} in the electrode.

Reopenings were observed at -70 mV following prepulses to +50 mV lasting ~200 ms. The distribution of open times showed two open states with mean lifetimes of 0.5 and 3 ms, similar to Ca^{2+} channels in other cells. The time before the first reopening into either short or long open state was measured at different repolarization potentials (-110 to -50 mV). The first latency changed little over a 60 mV range of membrane potentials, in contrast to the large change in first latency for activation, suggesting that the closed state prior to reopening is different from the normal resting closed state. We measured the probability of a reopening at negative potentials following prepulses to +50 mV of increasing duration. The probability of a reopening increased with longer prepulses, but reached a maximum of 40% with prepulses longer than 150 ms. The change in probability of a reopening as a function of prepulse length followed a time course that was indistinguishable from the decay of whole-cell Ca^{2+} current.

We suggest that strong depolarizations drive Ca^{2+} channels into an inactivated state from which they can reopen after repolarizing to negative potentials into either short or long open states. Rather than simply reducing Ca^{2+} influx, inactivation may enhance Ca^{2+} influx by capturing channels following voltage-dependent activation and releasing them for reopening at negative membrane potentials.

Th-AM-A4

INACTIVATION OF THE N-TYPE CALCIUM CHANNEL.

M. R. Plummer and P. Hess. *Dept. of Cellular and Molecular Physiology, Harvard Medical School, Boston, MA 02115.*

The whole-cell calcium current in rat superior cervical ganglion (SCG) neurons is carried primarily by N-type channels. (Plummer et al., Neuron 2: 1453 - 1463, 1989; Jones and Marks, J. Gen. Physiol. 94: 151 - 167, 1989). This N-type current inactivates slowly during voltage commands to positive potentials, and it has a large maintained component even after pulses of up to 500 ms in duration. Recordings of single N-type channels show a surprising dichotomy in the time course of inactivation (Fig.1). During 1400 ms pulses, the channel can burst briefly and then close for the remainder of the pulse, or it can burst for the entire duration of the pulse. In the experiment illustrated, short duration bursts (93 of 330 sweeps) occurred more frequently than long duration bursts (31 of 330 sweeps), but the pattern of bursting was non-random since the observed frequency of finding two successive bursts of the same type was significantly higher than predicted (short: 37 vs. 25.76; long: 9 vs. 2.7; X^2, $P < 0.05$ and 0.005, respectively). These observations cannot be accounted for by a linear kinetic scheme and suggest instead that the channel can switch between two modes of gating, one which inactivates rapidly, and one which does not.

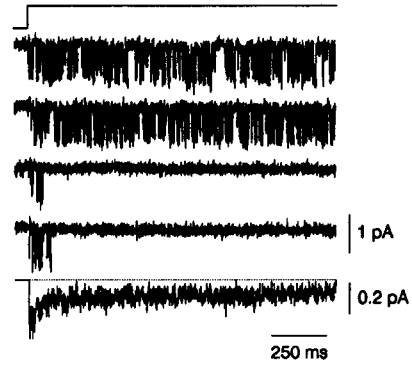

Fig. 1. Upper four sweeps: two patterns of inactivation from a recording of a single N-type channel. Bottom sweep: average current constructed from 120 idealized traces. Command potential: -90 mV to +20 mV. Pipette solution (in mM): 110 BaCl, 10 HEPES, 0.5 μM (+)-(S)-202791, pH 7.5. Bath solution: 140 KAsp, 10 HEPES, 5 EGTA, pH 7.5.

Th-AM-A5

THE DIFFUSION CONTROLLED ASSOCIATION STEP OF PERMEANT IONS WITH L-TYPE CA CHANNELS.

Chung-Chin Kuo and Peter Hess. Dept. Physiology and Program in Neuroscience, Harvard Medical School, Boston, MA 02115

The rate of entry of Ca ions into L-type Ca channels has been estimated as $4x10^8$ $(Msec)^{-1}$ (Lansman et al. JGP 88, 1986) under conditions where Ca is a blocker of monovalent currents through the channel. If this value described the rate of voltage independent diffusional access of ions to the channel (k_{on}), then a maximal current of -20 pA would be predicted with K as charge carrier if the relative aqueous diffusion coefficients for Ca and K ions are taken into account. Contrary to this expectation, we found that with 150 mM K as charge carrier (no divalent ions), the unitary inward current did not saturate at negative potentials and reached a value of -45 pA at -350 mV. The conductance increased from 120 at O mV to 230 pS between -200 and -300mV. This inward rectification was abolished by addition of 20% (Vol/Vol) glycerol, with no significant change of the conductance between 0 and -50 mV. In 30 % glycerol, the unitary currents saturated at a level of -25pS, with no more than a 10% increase between -250 and -350mV. This data suggests that the slowed aqueous diffusion of K-ions in the presence of glycerol unvails the voltage independent, diffusion controlled association rate of K-ions with the L-type Ca channel, with k_{on} = $1x10^9/(Msec)^{-1}$ in 30% glycerol. The value of k_{on} in water is expected to be 2.5 times faster than that in 30% glycerol (Andersen, BJ 41, 1983). The above calculation neglects a surface potential in the permeation path, an assumption which appears reasonable under our conditions but requires testing. The effective hemispherical capture radius $r=(k_{on}/2DN\pi)*10^3$ of the channel predicted from our data is 3.7 Angstrom, a value slightly larger than the radius (2.75 A) of the largest ion found to be permeable (McCleskey & Almers, PNAS 82, 1985). Even when the different diffusion coefficients for Ca and K are considered, our value of k_{on} remains higher than that for Ca block of Li currents by a factor of ~2.5. We suggest that this difference is due to competition between Li and Ca for channel occupancy. Thus we consider our value of k_{on} a closer estimate of the true diffusion limited association rate constant for ions with the L-type Ca channel.

Th-AM-A6

MOLECULAR DETERMINANTS OF ENSEMBLE AVERAGE CURRENTS CARRIED BY CALCIUM THROUGH L-TYPE CALCIUM CHANNELS.

William C. Rose, John P. Imredy, Eduardo Marban, David T. Yue, Depts. of Medicine and Biomedical Engineering, Johns Hopkins University, Baltimore MD.

Little is known about the gating kinetics of Ca channels when Ca carries charge. In particular, the kinetic processes involved in the inactivation of Ca current are not well characterized at the single channel level. We recorded unitary currents carried by 10 mM and 160 mM Ca through cardiac L-type Ca channels. The open probability during depolarizing pulses rose rapidly to a peak and then diminished. In 160 mM Ca the open probability fell to nearly zero by the end of 380 msec (figure 1, trace a). In 10 Ca the open probability declines less, maintaining a plateau for at least 160 msec (figure 2, trace a). Neither first latency nor open time can account for this difference in behavior, since the mean first latencies are very similar (25.3 vs 24.3 msec in high and low Ca respectively) and the mean open time is larger in high Ca. Despite inhomogeneous gating, convolution analysis can be used to gain insight into the genesis of ensemble currents because alteration in gating only begins after first openings (Yue et al., *Science*, in press). The convolution of first latency density (FL) with the open time histogram (OTH) falls far short of the ensemble average open probability (figure traces b), suggesting that channel reopening must account for much of the open probability, especially after the initial peak. We computed P_{oo}, the probability that a channel is open at a given time after it first opens. P_{oo} is the extension of the OTH to include reopenings, and P_{oo} will equal OTH if there are no reopenings. The convolution of FL with P_{oo} predicts well the ensemble average open probability (traces c). The different shapes of P_{oo} in high and low Ca give rise to the different shapes of the ensemble average open probability. In high Ca P_{oo} falls to near zero on a time scale which is rapid compared to the first latency; the convolution of FL with P_{oo} reflects the shape of the FL. In low Ca P_{oo} falls to a small nonzero plateau which is maintained throughout the pulse; the convolution of this P_{oo} with FL gives rise to a plateau which is not present in the FL. Thus the ensemble average open probability in high Ca reflects activation processes quite directly, while in low Ca the time course of open probability owes much to multiple late reopenings.

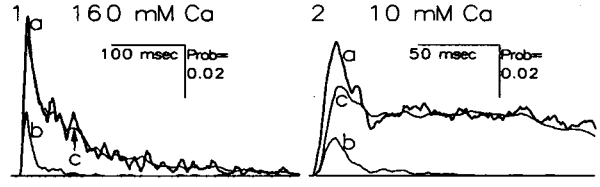

Th-AM-A7

PROPERTIES OF Ca^{2+} OSCILLATIONS IN BULLFROG SYMPATHETIC NEURONS.

D. D. Friel and R. W. Tsien, Molecular and Cellular Physiology, Stanford Medical Center, Stanford CA 94305

Sympathetic neurons have provided a useful model system for studying Ca^{2+} oscillations and the interplay between Ca^{2+} entry and Ca^{2+} release. We have studied oscillatory changes in $[Ca^{2+}]_i$ in intact bullfrog sympathetic neurons loaded with fura-2. $[Ca^{2+}]_i$ oscillations are observed in most cells when stimulated by a combination of high K^+ and caffeine but not by caffeine alone. It appears that oscillations involve caffeine-sensitive Ca^{2+} stores and Ca^{2+}-induced Ca^{2+} release (CICR): ryanodine (1 μM), which inhibits caffeine responses but has no detectable effect on Ca channel currents, abolishes the Ca^{2+} oscillations.

Each oscillatory cycle includes a slow rise in $[Ca^{2+}]_i$ leading to a Ca^{2+} spike with a rapid upstroke and a slower recovery. With $[K]_o$ fixed (usually at 30 mM), the characteristics of the $[Ca^{2+}]_i$ changes depend strongly on [caff]. In 1 mM caff, 30 mM K^+ produces a small, slow Ca^{2+} transient followed by a steady elevation in $[Ca^{2+}]_i$ but no oscillations. Increasing [caff] to 5 and then to 10 mM produces in succession an initial Ca^{2+} transient followed by repetitive spikes whose amplitude and period decreased with higher [caff]. This frequency increase is associated with acceleration of the slow Ca^{2+} rise, consistent with a caffeine-induced shift of CICR to lower $[Ca^{2+}]_i$. Finally, increasing [caff] to 30 mM produces another smaller [Ca] transient followed by a stable [Ca] elevation similar to that seen with 1 mM caff.

Sudden removal of high K^+ just after the upstroke leaves the ensuing Ca^{2+} spike unaffected, but abolishes the next slow Ca^{2+} rise; evidently, Ca^{2+} entry is not critical for an individual Ca^{2+} spike but is essential for the slow rise. Withdrawal of caffeine just after the upstroke causes an immediate fall of $[Ca^{2+}]_i$ and abolition of oscillations. Caffeine removal speeded the $[Ca^{2+}]_i$ fall at all stages of Ca^{2+} recovery, consistent with continued CICR pitted against Ca^{2+} uptake. Brief withdrawal of caffeine at various stages in the oscillation resets the oscillation; the earlier the withdrawal, the sooner the next spike. Caffeine withdrawal may promote refilling of caffeine-sensitive store or repriming of the Ca^{2+} release channel, thus hastening the next upstroke.

The potential for Ca^{2+} release during various phases of the oscillation was assessed by a sudden increase of [caff] to 30 mM. The 30 caff response was smallest just after the upstroke and grew progressively as $[Ca^{2+}]_i$ recovered and then slowly increased, reaching a maximum just before the next spike.

Th-Am-A8

VARIATION OF CA^{2+} CHANNEL SUBTYPE EXPRESSION IN DIFFERENT DIAMETER RAT DORSAL ROOT GANGLION NEURONS.

Reese S. Scroggs and Aaron P. Fox (Intro. by Rita Hice) Dept. of Pharmacological and Physiological Sciences, University of Chicago.

Small (20-27μm), medium (35-38μm) and large (45-51μm) diameter acutely isolated rat dorsal root ganglion (DRG) somata were treated with 2μM nimodipine and then 1μM ω-conotoxin GVIA (ω-CgTx) in order to determine the contribution to peak Ca^{2+} current (I_{Ca}) made by L and N Ca^{2+} channels, respectively, at a holding potential of -60mV. A larger percentage of I_{Ca} was blocked by nimodipine in small neurons (53% ± 4.7 SEM, N=11) than in large neurons (29% ± 9.2 SEM, N=10) (a,c). Medium neurons were usually insensitive to nimodipine (average decrease = 5% ± 3.3 SEM, N=10)(b). Subsequent treatment with ω-CgTx blocked a similar percentage of I_{Ca} in small (30% ± 3.8 SEM, N=11), medium (36% ± 4.0 SEM, N=9), and large (21% ± 2.1 SEM, N=9) neurons (a,b,c). However, a larger percentage of I_{Ca} was unblocked after treatment with ω-CgTx and nimodipine in medium neurons (55% ± 2.9 SEM, N=9) and large neurons (56% ± 7.7 SEM, N=9) versus small neurons (18% ± 2.7 SEM, N=11) (a,b,c). Rapidly inactivating low threshold Ca^{2+} currents evoked from holding potentials of -80mV to -100mV, (T channels), were present in small (N=10) and medium neurons (N=10), but were never observed in large neurons (N=10)(d,e,f). Low threshold Ca^{2+} currents evoked from medium neurons appeared considerably larger (4-6nA) than those evoked from small neurons (200pA-1nA) (d,e). The different diameter DRG somata may correspond to neurons which transmit different sensory modalities.

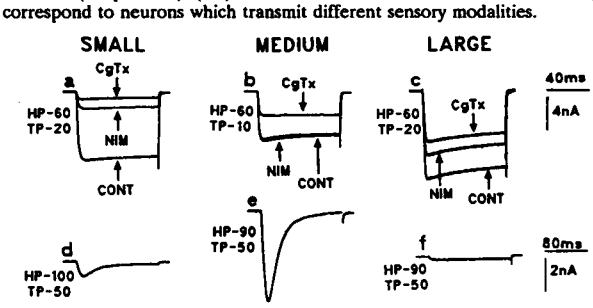

Th-AM-B1

LIGHT- AND POSITION-DEPENDENT FORMATION OF 3-D MEMBRANE CRYSTAL DOMAINS IN AMPHIBIAN CONE OUTER SEGMENTS (COS).

Joseph M. Corless and Ewa Worniallo. Departments of Cell Biology, Neurobiology and Ophthalmology, Box 3011, Duke University Medical Center, Durham, North Carolina 27710 USA

In COS, we have observed two classes of 3-D membrane crystals that are laterally continuous with disk domains of conventional morphology. (1) When bullfrog retinas are exposed to light, either *in vivo* or *in vitro*, crystalline domains are formed throughout the COS disk system. Such crystals may span 1-30 disks, and display (i) reduced disorder in lamellar organization, (ii) maintenance of intradisk spacing, and (iii) an increase (~8-10 nm) in cytoplasmic width compared to non-crystalline areas. The cytoplasm contains longitudinally or obliquely oriented densities, with lateral spacings of 11-13 nm. The intradiskal densities are rather punctate, with similar spacings. Crystal size and number increase with light exposure, and after 45 min in room lighting can occupy ~10% of COS volume *in vitro*. Such arrays may represent co-crystals between bleached opsin and one of the more abundant cytoplasmic proteins, e.g., transducin components or arrestin, and may contribute to the process of light adaptation. (2) In the salamander, *Amphiuma*, a different crystal type occurs almost exclusively along the closed margin segments of disks within the distal COS. Such crystalline domains usually involve 4-8 disks, and often show a periodic axial spacing of 18-20 disks. These crystals are characterized by nearly equivalent widths of the cytoplasmic and intradisk compartments (~9 nm), and by an array of short, axially oriented, filamentous densities within both compartments, but more readily visualized within the cytoplasm. In size, orientation and distribution, these filaments resemble those associated with the margins, incisures and preincisures of ROS disks. Their restriction to the distal half of the COS may result from a relative concentration of such components, induced by the progressive reduction in disk area associated with apical displacement of disks within the conical COS geometry.

Supported by NIH-NEI grants EY-04922 and EY-01659 to J.M.C.

Th-AM-B2

INFLUENCE OF MEMBRANE LIPID COMPOSITION ON MI-MII TRANSITION OF BOVINE RHODOPSIN.

Nicholas J. Gibson and Michael F. Brown (Intr. by H. Koffler). *Department of Chemistry, University of Arizona, Tucson, AZ 85721.*

Research in recent years points to a significant role of **lipid-protein interactions** in membrane protein function. Evidence increasingly suggests that the lipid headgroup size and charge and the acyl chain length and degree of unsaturation may contribute to protein function through modulation of the curvature and lateral compressibility of the membrane. These variables can be described in terms of the **lipid "average shape."** In the present work, lipid influences on bovine rhodopsin function were investigated by incorporating rhodopsin into vesicles of differing headgroup composition, while holding the acyl chain composition constant (at that of egg PC).[1] The MII/MI ratio produced by flash photolysis was determined as a function of pH to yield **titration curves** for the various recombinants. In addition, the influences of temperature were investigated. A native-like mixture of headgroup types was found to be necessary for optimum rhodopsin function, but was not sufficient to allow full native-like MII production. It has been suggested earlier that polyunsaturation of the lipid acyl chains is also necessary but not sufficient for full function.[2] Based on these pH titration results, an analysis of the relative contributions of the different headgroup types to rhodopsin function in native rod outer segment membranes is possible. [1]N.J. Gibson and M.F. Brown (1990) *Biochem. Biophys. Res. Commun.* **169**: 1028. [2]T.S. Wiedmann *et al.* (1988) *Biochemistry* **27**: 6469. Supported by NIH Grant EY03754.

Th-AM-B3

PHOTOTRANSDUCTION IN RODS AND CONES OF THE STRIPED BASS *(Morone saxatilis)*

James L. Miller and Juan I. Korenbrot, Department of Physiology, University of California, San Francisco, CA 94143

In order to understand the biochemical basis for the physiological differences in the response of rod and cone photoreceptors to light, one needs a preparation in which the rod and cone photoreceptors can be studied at both the biochemical and physiological level. The retina of the striped bass provides such a preparation and we have developed a method that separates isolated rods from cone photoreceptors. Using suction electrodes, we have characterized the light-response of rods and two classes of cone photoreceptors (singles and twins). The rods of the striped bass measure ca. 1.5 x 50 um and are maximally sensitive to light near 528 nm. The dim light response of bass rods reaches peak (t-peak) in 400 msec, the amplitude of the light response attains one half saturation following a light flash that delivers ca. 17 photons per um2, and the response to a light flash in the linear response range is reduced in amplitude by 50% in the presence of a background light of ca. 10 hV/um2-sec. The size of the cone photoreceptors depends upon the size of the animal and retinal location. The outer segment of the "average" single cone measures ca. 5 x 15 um, is maximally sensitive to light of ca. 540 nm, the t-peak is achieved in ca. 180 msec, the half-saturated photocurrent is produced by a flash density of ca. 100 photons/um2, and the response of these cells to a light flash within the linear response range is reduced by half by a background light of ca. 500 hV/um2-sec. The individual members of the twin pair are both maximally sensitive to light near ca. 605 nm and the outer segments of twins are generally larger than those of single cones. The photoresponse of each member of a pair is independent of its twin. Twins are both less sensitive (a half-saturating response is produced by a flash intensity of ca. 2000 hV/um2) and faster (t-peak ca. 100 msec) than single cones . Using a suction electrode, the cone photocurrent kinetics are distorted by the large capacitance of these cells (ca. 66 pf and 82 pf for singles and twins, respectively). Under voltage clamp, using tight-seal electrodes, the kinetics of the single cone remains slower than that of the twins (t-peak = 105 msec and 56 msec for singles and twins, respectively). For both cells, the kinetics of the photocurrent are voltage dependent. In general, as the voltage is depolarized, the onset kinetics and t-peak of the photocurrent are unchanged, but the decay phase of the response slows considerably. The current-voltage relation of the dark current is identical in both single and twin cones, exhibits outward rectification, and is identical to that measured in excised outer segment patches in the presence of cGMP. Supported by N.I.H. grants EY05617 to J.I.K. and EY06165 to J.L.M.

Th-AM-B4

BLOCK OF THE cGMP-GATED CHANNEL OF ROD AND CONE PHOTORECEPTORS BY L-cis-DILTIAZEM.

L.W. Haynes, Dept. of Medical Physiology, University of Calgary, Calgary, AB, T2N 4N1, Canada.

cGMP-gated channels in excised, inside-out patches were obtained from the outer segments of either catfish rods or cones or toad rods. Both sides of the patch were bathed in identical solutions containing 118 mM NaCl, 0.1 mM NaEDTA, 0.1 mM NaEGTA and 5.0 mM NaHepes (pH 7.6). Channels were activated by the addition of 1 mM cGMP to the bath and blocked by the application of micromolar concentrations of L-cis-diltiazem, a benzothiazapine, to the cytoplasmic or extracellular side of the patch. The current-voltage relation in the presence of blocker could be described at the macroscopic level by assuming that the blocker was impermeant and occluded the ion-conducting pore of the channel. The expected result of this block, inward-rectification, was in fact observed when diltiazem was applied to the cytoplasmic side of the channel. The dissociation constant at 0 mV for the cone channel in 12 patches averaged 16 ± 24 μM (mean ± sd) and decreased by e-fold over 51 ± 15 mV. The dissociation constant at 0 mV for the rod channel in 8 patches was significantly lower ($p < 0.05$), averaging 3 ± 1.4 μM, but the e-fold change over 60 ± 22 mV was not significantly different. In 4 cone patches containing only a single channel, the association rate constant at +30 mV averaged 7.5 ± 2.1 $\mu M^{-1}\ s^{-1}$ and the dissociation rate constant averaged 19 ± 6 s^{-1}. At -30 mV, the association rate decreased to 3.1 ± 2.6 $\mu M^{-1}\ s^{-1}$ and the dissociation rate increased to 30 ± 7 s^{-1}, giving e-fold changes over 69 mV and 123 mV, respectively. The concentration-dependence of block indicated a single diltiazem was sufficient to block the channel.

Block by diltiazem acting from the extracellular side of the channel was investigated by including 5 μM diltiazem in the recording pipet solution. The bath solution flowed rapidly across the cytoplasmic face to remove any diltiazem which might partition across the membrane. In this case, the expected result of either no block or outward rectification was not observed. Instead, inward rectification was again observed, a finding which is inconsistent with the idea that diltiazem acts by directly occluding the pore at the external side.

Th-AM-B5

INJECTION OF 1mM EGTA REVERSES DESENSITIZATION OF INOSITOL TRISPHOSPHATE-INDUCED CALCIUM RELEASE IN LIMULUS PHOTORECEPTORS. Richard Payne, Dept. Zoology, University of Maryland, College Park MD 20742.

Injection of inositol trisphosphate ($InsP_3$) into Limulus ventral photoreceptors causes a localized release of calcium from intracellular stores and an accompanying calcium-activated depolarization. The large $InsP_3$-induced elevation of Ca_i and the depolarization decline within 1-2s, but sensitivity to further injections of $InsP_3$ remains suppressed for 10-20s. This desensitization might be caused by depletion of calcium stores or by feedback inhibition of calcium release due to a small lingering elevation of Ca_i [Payne et al., 1990; Neuron 4, 547-555]. To distinguish between these possibilities, brief injections of 1mM EGTA and 100 μM $InsP_3$ were delivered through θ-glass micropipettes. The intention was to deliver sufficient EGTA after an injection of $InsP_3$ so as to remove any small, lingering elevation of Ca_i, but insufficient to antagonize the much larger elevation of Ca_i that would immediately follow any subsequent injections of $InsP_3$. To verify the latter, an injection of $InsP_3$ (duration 75ms) was delivered 750ms after a brief (300ms) injection of 1mM EGTA. The peak $InsP_3$-induced depolarization, which was used to monitor Ca_i, was not reduced relative to control values. Injection of higher concentrations of EGTA into other cells, however, did reduce the response to subsequent injections of $InsP_3$. The effect of 1mM EGTA on desensitization was next investigated by delivering an injection of EGTA between two injections of $InsP_3$ that were 1.5s apart. Without an intervening injection of EGTA, desensitization reduced the peak depolarization caused by the second injection of $InsP_3$ to 22±10% (S.E.; 5 cells) of control. However, an injection of 1mM EGTA, delivered 750ms after the first injection of $InsP_3$ restored the peak depolarization caused by the second injection of $InsP_3$ to 80±3% of control. Control injections of potassium aspartate into 6 other cells did not restore sensitivity to $InsP_3$. The major cause of the desensitization of calcium release therefore appears to be a lingering elevation of Ca_i and not depletion of calcium stores.

Th-AM-B6

LIGHT-ACTIVATED CHANNELS IN SCALLOP PHOTORECEPTORS: RECORDINGS FROM CELL-ATTACHED AND PERFUSED EXCISED PATCHES. E. Nasi and M. Gomez, Dept. of Physiology, Boston University School of Medicine and Marine Biological Laboratory, Woods Hole

On-cell patch clamp recordings were performed on the rhabdomeric membrane of solitary photoreceptors of Pecten irradians. Single-channel currents specifically activated by light were routinely obtained. The interaction of voltage with channel gating was examined using sustained voltage steps as well as ramps during steady-state channel activation by dim light stimulation. The frequency of light-induced openings increased markedly at depolarized potentials. Furthermore, at least one additional class of lower-conductance events was detected. The small-amplitude openings were infrequent, and usually appeared during the late phase of the photoresponse. Their occurrence did dot increase when a step of light was delivered under light-adaptation induced by dim background illumination. Several putative modulators of the light-dependent conductance were tested on excised patches previously screened for the presence of light-activated channels, but devoid of voltage-dependent channels. A double puffer-pipette was employed to locally perfuse the inner face of the patch with control intracellular solution and with test solutions. On several occasions a channel could be consistently activated by 100 μM 8Br-cGMP. However, fast flickering channel activity could also be induced by micromolar levels of calcium, while IP_3 induced the appearance of smaller channel events. The possibility of parallel light-dependent effector pathways suggests itself. Light-activated channels were also observed in isolated membrane patches, up to several minutes after excision, indicating that the complex enzymatic machinery of phototransduction was retained. This result calls for caution in attributing a direct gating role to substances applied to excised patches. Supported by NIH grant RO1 EY07559.

Th-AM-B7

EFFECTS OF LITHIUM, CALCIUM, AND PDE-INHIBITORS ON EXCITATION OF *LIMULUS* PHOTORECEPTORS. Peter M. O'Day, Edwin C. Johnson, & Marc Baumgard. Institute of Neuroscience, University of Oregon, Eugene, OR 97403, and Deptartment of Physiology, Marshall University School of Medicine, Huntington, WV 25706.

Phototransduction in *Limulus* ventral photoreceptors appears to involve both phosphoinositides (PI) and cyclic-GMP. IP_3-injection mimics light-induced excitation and Ca^{2+}-release. Channels opened by light in cell-attached membrane patches can be opened by cGMP in excised patches.

We have examined the roles of the cGMP- and the PI-pathways in excitation. We find: *A.* Prolonged exposure of photoreceptors to PI-pathway blocker, Li^+, slowed and reduced light-responses. This was reversible and preventable only by introduction of extracellular inositol. *B.* Light-induced Ca^{2+}-release was prolonged in low-Ca^{2+} (0.01mM) saline, suggesting that excitation *turnoff* is Ca^{2+}-dependent. *C.* In Ca_i^{2+}-stabilized cells, phosphodiesterase (PDE) inhibitors induced an inward current and greatly prolonged the light-response decay. *D.* The response decay to injection of slowly hydrolyzable 8-Br-cGMP was greatly slowed compared with cGMP. These effects were Ca^{2+}-sensitive. They suggest that response decay is governed by cG-PDE and cGMP synthesis occurs in the dark. *E.* Response time-courses were speeded and light response amplitudes were increased following bright illumination in some low-Ca^{2+} conditions (sensitization).

Our results are consistent with a channel ligand binding model of excitation in which response onset correlates with turn-on of ligand (cGMP) synthesis and binding, and decay correlates with ligand degradation. In this model: *(i)* the response waveform reflects synthesis and degradation of channel ligand, cGMP; *(ii)* ligand degradation is Ca^{2+}-sensitive; *(iii)* Ca^{2+}-release by IP_3 triggers ligand synthesis; *(iv)* light induces ligand synthesis *via* a pathway having two (at least) Ca^{2+}-sensitive parallel branches, one involving production of IP_3, the other unknown; *(v)* the ligand synthesis pathway is triggered by light, but its turn-off is Ca^{2+}-sensitive; *(vi)* release of Ca^{2+} by IP_3 stimulates ligand synthesis, ligand degradation, and the turn-off of ligand synthesis; *(vii)* ligand synthesis and degradation can persist following illumination. This model suggests that is insufficient to consider ligand synthesis in the absence of ligand degradation in modeling the light response in light-adapted cells. Supported by NSF BNS-8812455 & American Heart Association grants.

Th-AM-B8

PRIMARY STRUCTURE AND FUNCTIONAL EXPRESSION OF THE PUTATIVE HUMAN ROD PHOTORECEPTOR CYCLIC GMP-ACTIVATED CHANNEL, R.S. Dhallan[1,4], K.-W. Yau[2,4] and R.R. Reed[3,4], Depts. of Biomed. Eng., Neurosci.[2], Mol. Biol. and Gen.[3] and Howard Hughes Med. Inst.[4], Johns Hopkins Sch. of Med., Baltimore, MD 21205.

A cyclic GMP-activated channel is now thought to mediate visual transduction in vertebrate rod photoreceptor cells. We report here the molecular cloning, functional expression, and characterization of the putative cyclic GMP-activated channel in human rod photoreceptors. The coding region of the bovine rod cyclic GMP-gated channel (Kaupp et al., Nature 342, 762, 1989) was isolated and used to screen a human retinal cDNA library at low stringency. A partial cDNA clone was identified and was used to rescreen the library, giving a full-length cDNA clone. The putative protein encoded by this cDNA clone shares considerable homology (ca. 90% identity) to the bovine rod channel. Inside-out patches of plasma membrane from human 293 cells transfected with this putative human rod channel cDNA clone showed the expression of a cation channel that is activated by cyclic GMP and has properties very similar to those of the native rod channel in other species. Recently, Dryja et al. (Nature 343, 364, 1990) have reported that a point mutation of the rhodopsin gene may be the cause of one form of autosomal-dominant retinitis pigmentosa. It will be interesting to see if mutations in the human rod photoreceptor channel gene may be involved in other forms of retinitis pigmentosa.

Th-AM-B9

EXPRESSION OF SQUID RETINAL mRNA IN XENOPUS OOCYTES. B.E. Knox[1], D.A. Thompson[2] and E. Nasi[3] (Intro. by E.F. MacNichol). (1) SUNY HSC Syracuse (2) University of Michigan Medical School (3) Boston University School of Medicine and Marine Biological Laboratory, Woods Hole.

To define the signal transduction pathways operating in invertebrate visual cells, a characterization of the electrophysiological activities produced from photoreceptor mRNA has been undertaken using the Xenopus oocyte translation system. mRNA from squid retinae was prepared by guanidine HCl extraction and CsCl centrifugation. Poly A^+ RNA sizes up to 9.5 kb were obtained. In vitro translation using rabbit reticulocyte lysate produced a variety of proteins, with some polypeptides larger than 200 kDa. Stage V and VI Xenopus oocytes were injected with 5-10 ng mRNA and cultured for 48 to 96 hours. In response to depolarization above -20 mV, uninjected oocytes exhibit a transient outward current dependent on external calcium. mRNA-injected cells displayed significantly prolonged and enhanced currents (2-3 fold increase, 8 out of 10 oocytes). Upon repolarization to -60 mV, an increased inward tail current was also observed. mRNA-injected oocytes showed more than a 10-fold increased response to 2 μM ACh, which was abolished by 0.5 μM atropine. Serotonin did not evoke any response. The expression of light responsiveness in mRNA-injected oocytes was tested after incubation with 11-cis-retinal in the dark. Light induced sustained oscillatory inward currents ($\sim$ 100 nA, from a holding potential of -80 mV). The currents subsided when the light was turned off and were obtained repeatedly in the same oocyte. No light response was observed in any control oocytes incubated in 11-cis retinal, nor in mRNA-injected cells illuminated without retinal. Taken together, these observations indicate that the squid retinal mRNA preparation is intact, is capable of being efficiently translated and is able to direct the synthesis of proteins involved in light and neurotransmitter signal transduction. Supported by NIH grant RO1 EY07559.

Th-AM-C1

$[Ca^{2+}]_i$ TRANSIENTS IN CARDIAC MYOCYTES MEASURED WITH HIGH AND LOW AFFINITY CALCIUM FLUORESCENT INDICATORS. M. Konishi and J.R. Berlin. Bockus Research Institute. Philadelphia, PA.

To determine the accuracy of $[Ca^{2+}]_i$ transients measured in cardiac cells with high affinity calcium indicators, $[Ca^{2+}]_i$ transients in single rat ventricular myocytes were measured using fluorescent indicators with high, fura-2, and low Ca affinities, furaptra. Cells were voltage clamped with a single patch electrode and the K^+-salt of the indicator was loaded via the electrode. Changes in $[Ca^{2+}]_i$ with fura-2 were measured with a ratiometric method (340nm/380nm). In vitro calibration of fura-2 showed that resting Ca averaged approximately 60 nM while peak $[Ca^{2+}]_i$ resulting from a 50 msec voltage clamp depolarization from -70mV to +10 mV was approximately 400 nM. Determination of R_{min} and R_{max} in each cell with the Ca ionophore, 4-Br A23187 suggested that these levels of $[Ca^{2+}]_i$ could be underestimated by a factor of two. Calibration of $[Ca^{2+}]_i$ with furaptra was performed by measuring changes in fluorescence at 500nm during 370 nm illumination, correcting the fluorescence for movement artifacts and calculating changes in $[Ca^{2+}]_i$ as $\Delta F_{Ca:D} * K_d$ ($\Delta F_{Ca:D}$: change in the Ca^{2+} bound fraction of the indicator; K_d=47 μM). Resting $[Ca^{2+}]_i$ could not be calculated with this calibration method; however, the peak change in $[Ca^{2+}]_i$ averaged in excess of 2 μM. The time-to-peak $[Ca^{2+}]_i$ (approximately 35 msec) was similar for $[Ca^{2+}]_i$ transients measured with fura-2 and furaptra. Isoproterenol produced large increases in the $[Ca^{2+}]_i$ transient and increased the time to peak $[Ca^{2+}]_i$ observed with fura-2 but not with furaptra. These results suggest that fura-2 underestimates the size of the $[Ca^{2+}]_i$ transient in cardiac muscle compared to furaptra. This difference is not likely due to increased Ca buffering by fura-2 or Mg binding to furaptra during the $[Ca^{2+}]_i$ transient. Furthermore, the kinetics of Ca binding to fura-2 appear to be adequate only under limited experimental conditions.

Supported by Southeastern Pennsylvania Heart Assn. and HL43712

Th-AM-C2

BAPTA SELECTIVELY SUPPRESSES PEAK CALCIUM RELEASE IN FROG SKELETAL MUSCLE FIBERS. V. Jacquemond, M.G. Klein, L. Csernoch and M.F. Schneider, Dept. of Biological Chemistry, Univ. of Maryland School of Medicine, Baltimore, MD 21201

Resting $[Ca^{2+}]$ and calcium transients $\Delta[Ca^{2+}]$ were monitored in voltage clamped cut segments of single fibers containing both fura-2 and antipyrylazo III (AP III) in a double Vaseline gap (holding V = -100 mV, 3.8-4.5 μm/sarcomere, 8-10 °C). The rate of release (RREL) of Ca^{2+} from the sarcoplasmic reticulum (SR) was calculated from $\Delta[Ca^{2+}]$. BAPTA was pressure injected from a micropipette containing 0.5 mM fura-2, 10-50 mM BAPTA and $CaCl_2$ such that total pipette Ca:BAPTA = 1:10. In 5 fibers, 2.8-9.5 mM myoplasmic BAPTA (calculated from the increase in fura-2 fluorescence) lowered resting $[Ca^{2+}]$, virtually eliminated the AP III signal for 200 ms depolarizing pulses and considerably decreased the fura-2 fluorescence ratio signal. Before injection RREL had an early peak and then declined to a maintained level during the pulse. After injection the peak RREL was abolished. Assuming the SR calcium content to be unchanged by the injection, the steady level of RREL was about the same before and after injection (mean after/before ±SEM = 0.99 ± 0.29). Control injections of similar volumes of solution without BAPTA did not suppress peak RREL. The AP III and fura-2 signals recovered with time after injection as the injected BAPTA and fura-2 diffused out of the central region of the fiber, but the AP III signal during recovery had a much slower early rate of rise than before injection and the calculated RREL showed little recovery of the early peak. A possible direct pharmacological effect of BAPTA was not ruled out. However, the selective suppression of peak release after BAPTA injection may have been a slowly reversible result of buffered low $[Ca^{2+}]$, perhaps consistent with a role for Ca-induced Ca release before BAPTA injection.

Th-AM-C3

FAST DETECTION OF CA-TRANSIENTS ELICITED BY FLASH PHOTOLYSIS OF DM-NITROPHEN AND NITR-5 WITH THE FLUORESCENT INDICATORS RHOD-2 AND FLUO-3. Marino DiFranco*, B. A. Suárez-Isla# and J. Vergara. Department of Physiology, UCLA School of Medicine, *Fac. Ciencias, Universidad Central de Venezuela, Caracas, and #Dept. Fisiología y Biofísica, Fac. Medicina, U. de Chile.

The caged-Ca compounds DM-Nitrophen (Kaplan & Ellis-Davis, PNAS 85, 6571, 1988) and nitr-5 (Gurney et al. PNAS 84, 3496, 1987) were photolyzed by a 50 ns UV laser flash (340 nm) and the $[Ca^{2+}]$ transients were measured with the Ca-sensitive dyes rhod-2 and fluo-3. A tapered quartz optic fiber (tip diameter ca. 200 μm) was used to deliver UV flashes (frequency-doubled Ruby laser) to either flat microcuvettes, or single skeletal muscle fibers mounted on a triple vaseline-gap chamber, placed on the stage of an epifluorescence microscope. The high intensity laser pulses were delivered at 90° to the epifluorescence light path. The light collected by a 20x objective (N.A. 0.75) was focused on a photodiode; interference from stray illumination of the laser light was minimized with UV blocking filters. Experiments were performed in both cuvettes and muscle fibers using "internal" solutions containing (in mM) 110 K-ASP, 2 $MgSO_4$, 20 KMOPS, 5 ATP, 5 PCr, 0.1 μg/ml CPK, 20-50 μM rhod-2 or fluo-3 and 0.2-5 mM DM-nitrophen or nitr-5, pH 7.0. The pCa was adjusted in the range 8-6 with Ca electrodes.

In cuvette calibrations, the photolytic release of Ca^{2+} was rapidly tracked by the Ca dyes, displaying fluorescence increments with exponential rising phases that reached peak or steady values (depending on the conditions) with time constants between 0.5 to 3 ms (8-20°C). Laser-induced Ca^{2+} transients recorded from muscle fibers internally perfused with the same solutions, had magnitudes comparable to physiologically elicited Ca^{2+} transients, rising phases as fast as those observed in cuvettes, and were followed by a slower decaying phase. (We thank Drs. J. Kaplan and R. Y. Tsien for the kind gift of DM-Nitrophen and nitr-5, respectively. Supported by NIH AR-25201 and UCLA School of Medicine-BRSG).

Th-AM-C4

Increased Intracellular Calcium Mediated by Influx in Dystrophic Muscle. P.R. Turner, P.Fong & R.A.Steinhardt. Molecular & Cell Biology, U.C. Berkeley, CA 94720.

We have found elevations in free calcium ($[Ca^{2+}]_i$) in adult dystrophic mouse (mdx) muscle fibers (Turner et al, 1988), and in cultured dystrophic mouse and human myotubes (Fong et al, 1990), and shown that increased degradation in mdx muscle is related directly to $[Ca^{2+}]_i$. Calcium transients are longer in mdx fibers, suggesting that Ca^{2+} pump activity is impaired. When $[Ca^{2+}]_i$ levels were elevated to mdx levels in normal fibers, transient decay times at 25°C rose from 27 to 42 ms (n=6 fibers), and from 10 to 18 ms at 37°C (n=4). Conversely, mdx $T_{1/2}$ fell from 39 to 25 ms when $[Ca^{2+}]_i$ was pre-lowered to normal levels (n=8 fibers, 25°C), suggesting that the longer mdx transients result from the elevated $[Ca^{2+}]_i$, and not reduced pump activity. The $[Ca^{2+}]_i$ rise is not the result of a non-specific cation permeability increase, or voltage-gated calcium channel activity. Resting $[Na^+]_i$ levels (~9 mM, n=34), and initial Na^+ influx rates into mdx and normal fibers, measured using the dye SBFI, were identical. Influx rates were 1.07± 0.26 mM/min at 37°C (n=4), and 0.88 ± 0.20 mM/min at 25°C (n=13). Sodium influx rates in both normal and dystrophic myotubes were also identical (n=17, 25°C). The channel blockers nifedipine (5-50μM), verapamil (5 μM) and diltiazam (5 μM), did not lower $[Ca^{2+}]_i$ in mdx fibers (n=8). Sarcolemmal Ca^{2+} leak channels are more active in dystrophic myotubes (Fong et al, 1990). Channel densities are similar: single channels were found in ~50% of patches in each cell type. Nifedipine (10μM) increased normal mouse leak channel open probabilities 1.7 times, as well as $[Ca^{2+}]_i$ in normal mouse fibers by 13±2 nM (n=3) and in normal mouse myotubes by 25±5 nM (n=8). Larger increases occurred with 50 μM nifedipine. Thus increased leak channel activity can result in significant elevations in $[Ca^{2+}]_i$. We propose that the absence of dystrophin increases leak channel activity.

This work was supported by NIH and MDA.

Th-AM-C5

PHOSPHOLAMBAN MEDIATES THE RELAXANT EFFECT OF ß-ADRENERGIC AGONISTS IN MAMMALIAN VENTRICULAR MYOCYTES.

J.S.K. Sham, L.R. Jones*, and M. Morad. Dept. of Physiology, University of Pennsylvania, Philadelphia, PA 19104-6085, *Krannert Institute of Cardiology and Dept. of Medicine, Indiana University School of Medicine, Indianapolis, IN 46202.

The role of phospholamban in the regulation of sequestration of Ca^{2+} was studied in fura-2 loaded whole cell-clamped guinea-pig ventricular myocytes, using a monoclonal antibody (2D12) reacting only with phospholamban. The antibody stimulated Ca^{2+} uptake 5-fold in guinea-pig ventricular SR vesicles, shifting the apparent K_d for Ca^{2+} activation from 200 to 60 nM. The stimulatory effect of the antibody could be mimicked by the catalytic subunit of cAMP-dependent kinase, and could be blocked by phospholamban peptide 2-25. In ventricular myocytes, intracellular dialysis with 1 μM 2D12 for 12 to 15 minutes maintained SR Ca^{2+} loading at reduced extracellular [Ca^{2+}] (0.2 mM), in contrast to the great reduction in SR Ca^{2+} in control myocytes. The uptake of Ca^{2+} released by depolarizing pulses (from -60 to 0 mV) was also enhanced. The time-constant for uptake of Ca^{2+} estimated from fura-2 signal, was 385±91 msec in antibody-loaded myocytes compared to 697±111 msec in the control myocytes. Isoproterenol (0.3μM), which greatly enhanced the rate of release and uptake of Ca^{2+} in control myocytes, was much less effective in enhancing either the rate of release or uptake of Ca^{2+} in antibody-loaded myocytes. The enhancement of I_{Ca} by isoproterenol was not altered in antibody-loaded cells. We conclude that phospholamban regulates SR Ca^{2+} uptake in intact ventricular myocytes and that phosphorylation of phospholamban is sufficient to account for the enhanced rate of myocardial relaxation by ß-adrenoceptor stimulation. (Supported by NIH grant HL16152, HL28556, and HL06308.)

Th-AM-C6

GLUCONATE SUPPRESSES Q_β MORE EFFECTIVELY THAN Q_γ IN FROG CUT TWITCH FIBERS.

Wei Chen and Chiu Shuen Hui, Dept. of Physiology and Biophysics, Indiana University Medical Center, Indianapolis, IN 46223.

We reported the existence of normal Q_γ in some cut fibers with very little Q_β (Biophys. J, in press). This anomaly can be induced in a fiber with normal I_β by replacing Cl^- with gluconate. The inset shows an experiment in which a cut fiber was held at -90 mV in a 2-Vaseline-gap chamber. Charge movement was measured in a TEA.Cl solution first (left panel). Normal I_β and I_γ components can be seen in the ON-segments. When Cl^- was replaced by gluconate (right panel), I_β disappeared and I_γ was slightly suppressed. The Q-V plot in Cl solution can be fitted well by a sum of two Boltzmann distribution functions, representing Q_β and Q_γ, whereas that in gluconate solution does not show a Q_β component. The disappearance of Q_β was not due to a change in control charge because c_m measured between -110 and -90 mV remained practically constant; nor was it due to run-down of the fiber because the effect was mostly reversible. Averaged over six fibers, gluconate suppresses Q_β by 74% (±10%) and Q_γ by 22% (±6%). This implies that Q_γ is not tightly coupled to Q_β, as required in a sequential model for charge movement. Moreover, it rules out the possibility that Q_β is the trigger for Ca release and Q_γ is a consequence of the release (Supported by NIH NS21955 and a grant from MDA).

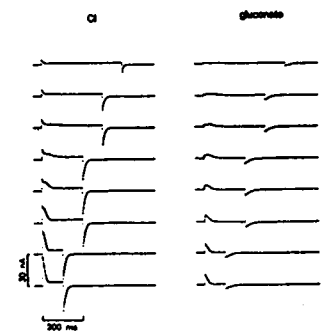

Th-AM-C7

DOES THE HUMP CHARGE MOVEMENT COMPONENT HAVE A NEGATIVE PHASE?

Chiu Shuen Hui and Wei Chen, Department of Physiol. and Biophys., Indiana University Medical Center, Indianapolis, IN 46223.

In the "feedback hypothesis" for Q_γ, the hump in charge movement traces is caused by Ca^{2+} released from the SR and binding to the inner surface of tubular membrane. If the depolarization is held sufficiently long for the Ca^{2+} to come off the membrane, an inward charge movement should follow. Such inward phase was reported (Pizarro, et al., Biophys. J. 57:341a, 1990). However, most of our fibers showing prominent I_γ humps did not show an inward phase, and when a dip in current occurred following the hump, it was limited to a very narrow potential range just above the threshold of Q_γ. The inset shows an experiment in which a cut fiber held at -90 mV in a 2-Vaseline-gap chamber was stimulated with test pulses (of durations 10-1000 ms) to -46 mV. The ON-current elicited by the 1 s pulse is shown in the upper panel of the inset and its running integrals in the lower panel, together with the OFF-charge (◇) from all the runs. Each running integral was obtained by using the correspondingly numbered baseline in the upper panel for correction. Only baseline #3 yields ON-charge that matches OFF-charge. This suggests that the dip following the hump cannot be due to inward charge movement but probably arises from the superposition of a decaying charge movement and a slowly rising ionic current (Supported by NIH NS-21955 and a grant from MDA).

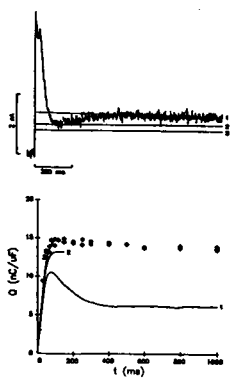

Th-AM-D1

EFFECT OF TEMPERATURE ON SODIUM-CALCIUM EXCHANGE IN SARCOLEMMA FROM MAMMALIAN AND AMPHIBIAN HEARTS

Malcolm M. Bersohn, Ramesh Vemuri, Duane W. Schuil, Roberta S. Weiss, Kenneth D. Philipson. Sepulveda and West Los Angeles VA Medical Centers and University of California, Los Angeles, CA

We investigated the temperature dependence of Ca^{2+} transport by the cardiac sarcolemmal Na^+-Ca^{2+} exchangers from dog, rabbit, and bullfrog hearts. The initial velocity of Na^+-Ca^{2+} exchange was measured as Na^+_i-dependent $^{45}Ca^{2+}$ uptake. In native rabbit sarcolemmal vesicles, the Ca^{2+} affinity of the Na^+-Ca^{2+} exchanger was the same from 7° to 37°, with the Km ranging from 22 to 26 μM. The velocity of Ca^{2+} uptake varied much more steeply with temperature below 22° than above 22°, with a sharp break in the Arrhenius plot at 22°. The calculated activation energy was 2 fold higher below 22°. In native dog sarcolemma, the temperature dependence of Na^+-Ca^{2+} exchange velocity was similar to that of native rabbit. In frog sarcolemma, the velocity of Na^+-Ca^{2+} exchange declined much more slowly with decreasing temperature at both temperature ranges. The calculated activation energies were 40-50% of those of the mammalian species at both temperature ranges. Reconstitution of the Na^+-Ca^{2+} exchanger into artificial lipid vesicles consisting of either asolectin or of phosphatidylserine, phosphatidylcholine, and cholesterol had little effect on the temperature dependence of Na^+-Ca^{2+} exchange velocity in any of the 3 species. The lesser temperature sensitivity of the cardiac sarcolemmal Na^+-Ca^{2+} exchanger of bullfrogs is appropriate for a poikilothermic existence. Because the difference from mammalian species remained after reconstitution, it appears to be an intrinsic property of the transport protein.

Th-AM-D2

CYTOPLASMIC ACIDITY INHIBITS SODIUM-CALCIUM EXCHANGE IN CARDIAC CELLS.

Doering, A.E. and Lederer, W.J.
Dept. of Physiology, University of Maryland School of Medicine, Baltimore, MD.

Sodium-calcium exchange is the principal mechanism of intracellular calcium extrusion in mammalian heart muscle. We measured outward sodium-calcium exchange current in giant membrane patches excised from guinea pig cardiac myocytes (Hilgemann, Nature 344:242, 1990; Pflugers Archiv 415:247, 1989). Adult ventricular cells incubated overnight in 135 KCl develop membrane blebs. A giant patch pipette (10 μm tip) is sealed to a bleb and lifted to excise an inside-out patch. The pipette solution contains (in mM) 140 NaCl, 40 N-methyl glucamine (NMG), 10 TEACl, 20 PIPES, .020 EGTA, 1 $CaCl_2$, .025 ouabain, .0025 D-600, and 1 4-AP. In the bath is 140 NMG, 10 TEACl, 5 ATP, 1 $MgCl_2$, 20 PIPES, 20 BAPTA, and 0.3μM free Ca^{++}. Rapid solution changes are achieved using an oil-gate chamber (Qin and Noma, Am. J. Physiol. 255:H90, 1988). The figure below shows the outward current activated when the cytoplasmic solution is changed from 0 NaCl to 60 NaCl at pH 7.2. The same step change in NaCl at pH 6.4 induces a current with different kinetics and a reduced steady-state level. The latter result agrees with earlier work showing that decreased pH_i inhibits Na-Ca exchange (Mullins, et.al., J. Physiol., 1983, 338:295). The degree of steady-state block decreases at sodium concentrations greater than 60mM and may reflect hydrogen ion competition for Na binding sites on the exchanger.

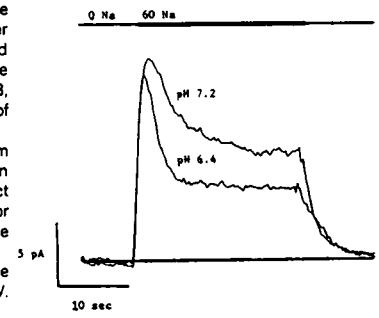

We gratefully acknowledge the assistance of Dr. D. W. Hilgemann.

Th-AM-D3

CHANGES IN THE AMPLITUDE OF Na-Ca EXCHANGE CURRENT FOLLOWING TWITCHES IN GUINEA PIG VENTRICULAR CELLS.

Thomas K. Chin, Kenneth W. Spitzer and John H.B. Bridge. Division of Pediatric Cardiology and the Nora Eccles Harrison CVRTI, University of Utah, Salt Lake City, UT 84112

A rapid perfusion method has recently been used to measure electrogenic Na-Ca exchange in cardiac myocytes (Bridge et al, 1990, Science 248:4953; Chin et al, 1990, J Gen Phys 96:40a). In this study, changes in peak amplitude of Na-Ca exchange current ($I_{Na\text{-}Ca}$) were observed following presumed alteration in Ca_i. Freshly isolated ventricular myocytes obtained by enzymatic digestion were studied at 23°C. Cells were voltage-clamped and held at -40 mV with microelectrodes containing Cs and deficient in Na. Ca current (I_{Ca}) was activated by depolarizing the cell with an 80 ms clamp pulse to +10 mV in the absence of Na (Li replacement), which produced a twitch. Rapid application ($t_{1/2}$ =2 ms) of 145 mM Na activated $I_{Na\text{-}Ca}$. When we applied Na at increasing time intervals after the clamp pulse, peak $I_{Na\text{-}Ca}$ declined at a rate which approximated the time course of $I_{Na\text{-}Ca}$, (and also presumably reflects the time course of Ca transients). If Na was applied after 1-5 conditioning pulses in 0 mM Na (when contractions and presumably Ca_i were larger), the amplitude of $I_{Na\text{-}Ca}$ increased from 10% to 30% of I_{Ca} and returned to baseline in 2-3 beats. Further, prolongation of the pacing interval resulted in a steady-state increase in I_{Ca} and an associated increase in $I_{Na\text{-}Ca}$. These results suggest that changes in the amplitude of $I_{Na\text{-}Ca}$ reflect alterations in Ca_i, and may be used to measure the time course of Ca transients. We infer that the magnitude and time course of $I_{Na\text{-}Ca}$ is determined by the rise and fall of cytosolic Ca (which is primarily regulated through Ca release and sequestration by the sarcoplasmic reticulum). [Supported by NIH grants HL-42357 and HL-42873; the Nora Eccles Treadwell Foundation and the Richard A. and Nora Eccles Harrison Fund for Cardiovascular Research].

Th-AM-D4

NA/K PUMP SITES INDUCED BY LOW K IN VOLTAGE CLAMPED CULTURED CHICK CARDIAC MYOCYTES.

J. R. Stimers*, S. Liu# and M. Lieberman+, *Department of Pharmacology & Toxicology and #Division of Cardiology, University of Arkansas for Medical Sciences, Little Rock, AR, and +Department of Cell Biology, Division of Physiology, Duke University Medical Center, Durham NC.

Embryonic chick cardiac myocytes cultured for 24 h in normal 5.4 mM K (NK) and low 0.5 mM K (LK) medium were used to study the Na/K pump. In a previous study, under LK conditions chick cardiac myocytes undergo an increase in Na/K pump sites as indicated by an increase in ^{3}H-ouabain binding sites (Lobaugh and Lieberman, 1985, *J. Gen. Physiol.* 86:31a). In this study we ask whether these increased Na/K pump sites are functional and do they have the same properties as Na/K pumps in control preparations. Using the whole-cell patch-clamp technique, single cardiac myocytes were voltage clamped at -70 mV to record the ouabain sensitive Na/K pump current (I_p). Ca-free HEPES bufferd salt solution with 1 mM Ba, 0.1 mM Cd and 10 mM Cs was used to minimize other membrane currents. Varying Na in the pipette (intracellular) solution from 6 - 51 mM revealed that the Na-dependence of I_p was similar in both control and LK preparations; however the current magnitude was increased about 30-50%. Similar results were obtained when extracellular K was varied from 0.3 to 10.8 mM. Apparent affinity was not significantly affected while I_p magnitude was increased in LK myocytes. However, the apparent affinity for ouabain was decreased from 3 μM in NK to 6 μM in LK preparations. These results suggest that while the induced Na/K pumps may behave similarly under physiological conditions, there sensitivity to ouabain is decreased. This suggests that chick cardiac myocytes may contain more than one isoform of the Na/K pump that can be differentially expressed. Supported in part by NIH grants HL27105 and HL44660.

Th-AM-D5

THE EFFECT OF INTRACELLULAR pH ON PHASIC CHANGES OF MYOCARDIAL SODIUM CURRENT. Michael R. Gold and Gary R. Strichartz,(sponsored by Sukumar Desai) Brigham and Women's Hospital Anesthesia Research Laboratories and Harvard Medical School, Boston, MA.

Repetitive depolarization of the myocardial membrane produces a phasic decrease in peak sodium current (I_{Na}), which is due largely to the slow reactivation process of I_{Na} in this tissue. The resulting conduction slowing may be important in the genesis of arrhythmias. Because intracellular acidification is an early event during myocardial ischemia we investigated the effect of intracellular pH (pH_i) on slow reactivation. Cultured chick myocytes were perfused internally with buffered solutions of pH 6.2-7.7 while I_{Na} was measured by the whole-cell patch clamp method. The effect on peak I_{Na} of repetitive depolarization from −100 to 0 mV was studied in 13 cells in the presence of amiloride (300 μM) to block Na-H exchange. At 2 Hz, the steady state decreases of I_{Na} (as % of 1st pulse current) were 24±4, 28±6 and 21±2 for pH_i's of 6.2, 6.7, and 7.2, respectively. This decrement of I_{Na} was frequency dependent (increasing from 1 to 3 Hz) and was abolished at all pH_i by increasing the holding potential to −140 mV. Reactivation at −100 mV after a 150 msec depolarization to 0 mV was also measured in an additional 30 cells. Reactivation kinetics were described best as a biexponential function, with 75% of I_{Na} recovering rapidly (τ_f ~ 80 msec) and the remainder recovering slowly (τ_s ~ 420 msec). Neither recovery phase was affected by pH_i (p>0.1). It is concluded that intracellular acidification is probably not a mediator of ischemic-induced conduction slowing and arrhythmias. Supported by USPHS grant GM15904

Th-AM-D6

COMPLEX CHARACTERISTICS OF STEADY-STATE TTX-SENSITIVE BACKGROUND SODIUM "WINDOW" CURRENT IN CANINE CARDIAC PURKINJE FIBERS. Gary A. Gintant, Masonic Medical Research Laboratory, Utica NY. 13501

A steady-state background inward sodium "Window" current ($I_{Na,Window}$) helps sustain the action potential plateau and modulated action potential duration in cardiac Purkinje fibers. $I_{Na,Window}$ is postulated to result from the overlapping voltage dependence of the activation (m) and inactivation (h) gates of fast sodium channels, and thus should be an inward current at potentials negative to the sodium equilibrium potential(E_{Na}). To further study $I_{Na,Window}$, shortened canine cardiac Purkinje fibers were voltage-clamped (2 microelectrode technique,37° C); $I_{Na,Window}$ was assessed as the difference (Control-TTX) in currents obtained during identical depolarizing ramps (≤10 mV/sec) in the absence vs. presence of TTX (≤ 2×10^{-5} M). In some fibers, $I_{Na,Window}$ was inward at negative potentials, but unexpectedly crossed to become outward at potentials far below the expected E_{Na}, sometimes at potentials as negative as -30 mV. For any given ramp potential, the amplitude of either inward or outward $I_{Na,Window}$ increased with greater TTX concentrations, reaching a maximum near 2×10^{-5} M TTX. As beta-adrenergic stimulation may modulate fast sodium current, we also assessed its effects on $I_{Na,Window}$. Isoproterenol (≤ 1 μM) increased net outward current at all potentials during depolarizing ramp pulses, with a maximum in the range of -25 mV. Isoproterenol did not affect the maximum amplitude of TTX-sensitive inward $I_{Na,Window}$, but sometimes elicited additional TTX-sensitive current between -30 to -10 mV. Thus, in contrast with earlier interpretations, $I_{Na,Window}$ may be either inward or outward at plateau potentials in some fibers, and is minimally affected by beta-adrenergic stimulation. $I_{Na,Window}$ likely plays a role in the generation of repolarization abnormalities, including early afterdepolarizations.

Th-AM-D7

MECHANISM OF BLOCK OF NA CHANNELS BY BIDISOMIDE: EFFECTS ON INACTIVATION. C.L. Martin and K. Chinn (Intro. by T. Narahashi). Searle, Skokie, IL 60077.

Bidisomide (SC-40230), a class I antiarrhythmic agent (Na channel blocker) now in clinical trials, was found to reduce Vmax (maximum dV/dt of the upstroke of the action potential, an indirect measure of Na current) in a frequency-independent manner in guinea pig papaillary muscle. (Martin et al, Drug Dev. Res.17:51-61;1989). The onset of drug-induced Vmax reduction was relatively slow (12 action potentials required to reach 63% of steady state reduction at 1 and 3.3 Hz), but the recovery process was extremely slow (τ = 8 min, Martin and Chinn, The Pharmacologist. 32:17;1990). The action potential data showed that Vmax reduction occurred after repetitve stimuli. There was no reduction of the first Vmax value, obtained after drug exposure and therefore probably no block of rested state Na channels. We examined the effects of bidisomide at the whole cell level to obtain a better idea of the mechanisms by which the channels became non-conducting. To determine whether block occurred in the open or inactivated state, the time spent in the inactivated state was increased by increasing the stimulus pulse duration (from 40 ms to 400 ms). Both the time constant of block development and steady state block were similar at both durations, indicating that block during the inactivated state was not a major factor. We also examined whether bidisomide altered the inactivaton current voltage curve (h_∞). At 3 and 30 μM, bidisomide shifted the curve to more negative voltages by at least 10-20 mV. This was probably an underestimate due to the presence of normal as well as drug bound channels in producing the curve. We have thus found that 1) block by bidisomide occurs primarily in the open state and not the inactivated state, and 2) bidisomide shifts the h_∞ curve to negative voltages, and consequently the number of channels available to open at normal resting potentials is reduced.

Th-AM-D8

A CALCIUM-ACTIVATED CHLORIDE CURRENT IN RABBIT VENTRICULAR AND ATRIAL MYOCYTES. Andrew C. Zygmunt and W.R. Gibbons, Dept. of Physiology and Biophysics, Univ. of Vermont College of Medicine, Burlington, VT 05405.

We have examined the ionic basis of a transient outward current in rabbit myocytes. Cells were voltage clamped by the whole cell patch clamp technique. Sodium channel currents and Na-Ca exchange were blocked by 20 uM TTX and removal of sodium from bath and pipette solutions. Depolarization of ventricular cells to potentials positive to -20 mV resulted in slowly decaying outward current. A portion of this current was blocked by 2 mM 4-aminopyridine (4AP); the 4AP sensitive current appeared equivalent to previously described transient outward potassium current in heart. In the presence of 4AP, a small second outward current was revealed that peaked in 20 ms and decayed within 100 ms. Isoproterenol potentiated the 4AP resistant transient current; cadmium or nisoldipine blocked it. The 4AP resistant transient current was blocked by ryanodine, by caffeine, or by high concentrations of intracellular calcium buffer, each of which reduces intracellular calcium transients. These data are consistent with a current activated by the calcium transient that causes contraction. The current was not abolished by the potassium channel blockers 4AP, tetraethylammonium, charybdotoxin, or apamin, and was still present if external potassium was omitted and internal potassium was replaced by cesium. The current was absent when extracellular and intracellular chloride were drastically reduced. The current was blocked by the anion transport blockers SITS and DIDS. Thus chloride appeared to carry the 4AP resistant transient current.

Rabbit atrial myocytes also have two transient outward currents, one of which is insensitive to 4AP. We have subjected the 4AP insensitive current of atrial cells to most of the tests performed on ventricular myocytes, with equivalent results. Thus, we conclude that the 4AP resistant transient outward current of rabbit atrial and ventricular myocytes is a calcium-activated chloride current. (Supported by HL14614 and HL07647)

Th-AM-D9

MECHANOSENSITIVE ION CHANNELS IN ATRIAL MYOCYTES D.R. Van Wagoner, Research Institute, Cleveland Clinic Foundation, Cleveland, OH 44195-5069.
Mechanosensitive ion channels have been observed in a wide variety of tissues and species, but there has been no detailed study reported on their distribution in the mammalian heart. In experiments in my laboratory, I have discovered a stretch-activated, non-selective cation channel in the membrane of atrial myocytes obtained from either neonatal or adult rats. This channel has been observed in 20-30% of the cell-attached patches ($n > 200$) studied. With lower frequency, I have observed a stretch inactivated potassium selective ion channel in these cells. The administration of negative pressure (5-50 mm Hg) to patches of atrial cell membranes resulted in either: 1) an increase in the open probability of the stretch-activated channels, or 2) a dramatic inhibition of the stretch-inactivated potassium channel activity. These types of channels were detected in both freshly isolated neonatal and adult myocytes, as well as in neonatal myocytes maintained in culture for up to three weeks. The stretch-activated cation channels are not highly selective for Na^+ or K^+ ions, with a slope conductance of 170 pS in 140 mM K-acetate, and 94 pS in 140 mM Na-acetate.

While not previously identified in atrial myocytes, mechanosensitive channels may play an important role in modulating the rate and force of atrial contraction, as well the secretion of atrial natriuretic factor (ANF). This study demonstrates the existence of at least two unique types of mechanosensitive ion channels in rat atrial myocytes. The distribution and functional significance of these channels are currently being explored. Supported by the Northeast Ohio AHA.

Th-AM-E1

DIRECT DETERMINATION OF ACYL CHAIN PACKING IN LIQUID-CRYSTALLINE BILAYERS FROM COMBINED NEUTRON AND X-RAY DIFFRACTION DATA. Michael C. Wiener and Stephen H. White. *Department of Physiology and Biophysics, University of California, Irvine, CA 92717.*

The average packing of the hydrocarbon interior of lipid bilayers is believed to be similar to the packing of liquid alkanes although their detailed conformations differ. This correspondence is based upon a variety of observations and calculations, notably the similarity of liquid-crystalline lipid and liquid alkane wide-angle diffraction patterns. We have developed procedures for the determination of detailed liquid-crystalline bilayer structures by the joint refinement of neutron and x-ray lamellar diffraction data (Wiener and White, *Biophysical Journal*, in press). The refinement procedure utilizes "quasi-molecular" structural models where the bilayer unit cell is divided into a series of multiatomic (quasi-molecular) fragments. This refinement procedure leads directly to a determination of the terminal methyl distribution and the average packing of the bilayer interior. For typical lipids, the bilayer interior is composed primarily of methylene and terminal methyl regions. By combining bilayer Fourier profiles obtained from neutron and x-ray structure factors that are on absolute scales, the real-space profiles of the terminal methyl and methylene regions near the center of the bilayer are determined directly for L_α DOPC. The methyl distribution is well-approximated by a Gaussian function. Combining these distributions with the average lipid area obtained from volumetric measurements leads to determination of CH_2 and CH_3 volumes in liquid-crystalline bilayers. These values are similar to CH_2 and CH_3 volumes of liquid alkanes. (Supported by NIH grant GM37291 and NSF grant DMB880743).

Th-AM-E2

ANGULAR DEPENDENCE OF DEUTERIUM SPIN-LATTICE (R_{1Z}) RELAXATION RATES OF MACROSCOPICALLY ORIENTED PHOSPHATIDYLCHOLINE BILAYERS. Theodore P. Trouard and Michael F. Brown. *Department of Chemistry, University of Arizona, Tucson, AZ 85721.*

Deuterium (^2H) NMR has been commonly used to determine the types and rates of motions that exist in lipid bilayers. Recently, the orientation dependence of the spin-lattice (R_{1Z}) relaxation rates of various systems has been measured in order to test proposed motional models. Values of R_{1Z} were determined for macroscopically oriented bilayers of di(per-^{2}H-12:0)PC and di(per-^{2}H-14:0)PC in the liquid-crystalline state at various values of the angle β between the bilayer normal and the magnetic field. Angle dependent profiles of R_{1Z} along the entire lipid acyl chains were obtained. A small angular anisotropy was observed in both systems in which $R_{1Z}(0^o) < R_{1Z}(90^o)$. The anisotropy of R_{1Z} was greater for the segments nearest the aqueous interface, which possess larger values of S_{CD}, than those closer to the middle of the bilayer. The angular dependence of the relaxation was then used to test three general types of models which account for the molecular dynamics.[1] These include (i) *fast segmental motions* of the acyl chains as well as two types of slow motions which modulate the electric field gradient tensor preaveraged by faster motions, *viz.* (ii) *molecular motions* (non-continuum model)[2] and (iii) *collective director fluctuations* (continuum model). [1]M.F. Brown and O. Söderman (1990), *Chem. Phys. Lett.* **167**, 158. [2]M.F. Brown (1990), *Mol. Phys.*, in press. Work supported by the NIH (GM41413, EY03754, and RR03529).

Th-AM-E3

MODULATION OF THE ORIENTATIONAL ORDER PROFILE OF THE LIPID ACYL CHAIN IN THE L_α PHASE

M. LAFLEUR[1,3], P. R. CULLIS[1] and M. BLOOM[2]
[1]Department of Biochemistry and [2]Physics Department, University of British Columbia, Vancouver B.C., V6R 2X7, [3]Département de chimie, Université de Montréal, Montréal (Québec), H3C 3J7, CANADA.

The orientational order profile along the lipid acyl chain has been characterized under several different conditions of polar headgroup composition, temperature, and cholesterol content, using ^2H NMR. Despite the different nature of these factors, the variation of the order is governed by two common trends. First, the relative change of order induced by the variation of these factors is always more pronounced towards the end of the chain than for the methylene groups near the interface. Second, there is, to a first approximation, a distinct correlation between the magnitude of the order parameters and the shape of the order profile. For example when the chain is highly ordered, the relative width of the order distribution is narrow indicating that the plateau region is longer. These conclusions suggest that the orientational order profile depends on only a small number of parameters and demonstrate clearly that the correlation length for changes in orientational order is much greater than one C-C bond length.

Th-AM-E4

NEW RESULTS IN THEORY OF HYDRATION FORCES: THE ROLE OF SURFACE STRUCTURE OF LIPID MEMBRANES, DEHYDRATION TRANSITION.

S. Leikin[a,b], A. A. Kornyshev[b]
(Intro. by C. R. Moore)
(a) *PSL/DCRT & LBM/NIDDK, National Institutes of Health, Bldg. 10, Rm. 9B-07 Bethesda, MD 20892*; (b) *The A. N. Frumkin Institute of Electrochemistry, Acad. Sci. USSR, Moscow, USSR*

In recent years detailed experiments have shown that the decay length of the hydration repulsion is strongly dependent on the structure of the interacting membranes. Evidence of the hydration attraction, leading in some cases to full dehydration of the membranes, has also been found. These features of the hydration forces could not be described by the existing theories. In the present work we show that the main features of the hydration force between neutral phospholipid membranes are determined by the intra- and inter-surface spatial correlations in the distribution of the hydrated groups on the membrane surface. When polar heads of lipid molecules are disordered the hydration force is purely repulsive. With the increase of the lateral intra-surface ordering, the decay length of the force decreases and the preexponential factor increases. When ordering reaches a critical value, the inter-surface correlations become strong enough to provide a dehydration transition, i.e. the formation of the dehydrated contact between the membranes. Our theoretical predictions explain the observed dependence of the force parameters on the surface structure as well as some very peculiar phenomena such as *strengthening* of the force with *decreasing* surface density of the polar heads. This strengthening occurs upon the melting of lipid hydrophobic chains or the mixing of lipid molecules with molecules of diacylglycerol.

Th-AM-E5

STRUCTURE, THERMAL PROPERTIES, AND INTERBILAYER INTERACTIONS OF SPHINGOMYELIN:CHOLESTEROL AND SPHINGOSINE:CHOLESTEROL BILAYERS. T. J. McIntosh[1], S. A. Simon[2], and C. Huang[3]; Dept. of Cell Biology[1] and Neurobiology[2], Duke Univ. Medical Center, Durham, N.C. and Dept. of Biochemistry[3], Health Sciences Center, Univ. of Virginia, Charlottesville, Va.

Sphingomyelin (SM) is a component of many plasma membranes and sphingosine (SS) is a sphingolipid breakdown product that inhibits protein kinase C, an enzyme involved in cell regulation. These two lipids are invariably found in membranes with high concentrations of cholesterol. We observe that both SM and SS interact strongly with cholesterol. The progressive addition of cholesterol reduces the transition enthalpy of both SM and SS bilayers, until no transition is observed at about 50 mol % cholesterol for SM and about 33 mol % for SS. X-ray diffraction shows that the incorporation of cholesterol fluidizes the hydrocarbon chains of gel phases of both SM and SS bilayers. In the case of synthetic sphingomyelin with a saturated acyl chain of 24 carbons, the lipid methylene chains interdigitate in the absence of cholesterol. Cholesterol reduces the extent of this interdigitation as it packs into the hydrocarbon chain region near the SM headgroup and fluidizes the methylene chains near the center of the bilayer.

For interbilayer separations from 5 to 20 Å, the hydration pressure for both SM and SM:cholesterol bilayers decays exponentially with increasing fluid space with a decay length of about 2 Å. This decay is similar to that observed for phosphatidylcholine (PC) and PC:cholesterol bilayers. For all of these bilayers containing PC and SM, the magnitude of the hydration pressure is proportional to the square of the Volta potential as measured for monolayers in equilibrium with liposomes. For SM bilayers, as for PC bilayers, there is an upward break in the pressure-distance relation at an interbilayer spacings of ~ 5 Å, probably indicating the onset of steric repulsion betwen the headgroups of apposing bilayers.

Th-AM-E6

ANTIBODIES TO ACETALDEHYDE-PROTEIN ADDUCTS BIND TO ACETALDEHYDE-PHOSPHATIDYLETHANOLAMINE ADDUCTS IN HEXAGONAL PHASE MICELLES BUT NOT IN LIPOSOMES

James R. Trudell, Ph.D., Department of Anesthesia, Stanford University, Stanford, CA 94305-5123

These studies measured the binding of hapten-specific IgG antibodies purified from the sera of rabbits sensitized to an albumin-acetaldehyde conjugate (N-ethyl-RSA) to acetaldehyde-dioleoylphosphatidylethanolamine adducts (N-ethyl-DOPE). Lamellar liposomes containing either 5% by weight N-ethyl-DOPE and 95% egg phosphatidylcholine or a mixture of 5% N-ethyl-DOPE, 24% DOPE and 71% dioleoylphosphatidylcholine (DOPC) as well as hexagonal phase micelles containing 5% N-ethyl-DOPE and 95% DOPE were prepared by sonication. Anti-N-ethyl-RSA IgG antibodies were then incubated with each of these lipid mixtures for 30 min, a fluorescein conjugated goat anti-rabbit IgG antibody was added for an additional 30 min, and then binding to the liposomes or micelles was measured by flow cytometry. The affinity of anti-N-ethyl-RSA IgG antibodies was 16 times greater for the hapten in the hexagonal phase. A second set of experiments were performed to determine if there are domains on the surface of hepatocytes that expose haptenic phospholipids to antibodies in a manner similar to the surface of hexagonal phase micelles. Liposomes containing N-ethyl-dioleoyl-phosphatidylethanolamine were fused with isolated hepatocytes, the affinity purified primary IgG antibodies and then fluorescein-conjugated second antibodies were added, and antibody binding to hepatocytes was measured by flow cytometry. The fluorescence of these hepatocytes was significantly greater ($P < 0.01$) than control hepatocytes prepared with (a) pre-immune primary IgG antibodies with fluorescein-conjugated second antibodies, (b) no primary antibody but with fluorescein-conjugated second antibodies, and (c) no fluorescein-conjugated second antibodies. These results demonstrate that the environment of a hapten can affect antibody recognition and that domains similar to the surface of hexagonal phase micelles exist on the surface of hepatocytes.

Th-AM-E7

DUAL EFFECT OF BLEOMYCIN ON PHOSPHATIDYLETHANOLAMINE VESICLES Sanda Clejan & Cheri Yost, Tulane University Medical Center, New Orleans.

The antitumor drug bleomycin (BLM) produces acute lung injury and pulmonary fibrosis. The effect of BLM on phosphatidylethanolamine (PE) lipid polymorphism has been studied by means of differential scanning calorimetry, ^{31}P-NMR and leakage of carboxyfluorescein (CF) from vesicles. Incorporation of increasing amounts of BLM results in a progressive decrease of both transition temperature and enthalpy, part of the PE molecules, (those interacting with BLM) give rise to a broad bilayer to hexagonal phase transition (H_{II}) which is shifted to lower temperatures. The remainder of the PE still shows a slightly perturbed transition. This interpretation was confirmed by ^{31}P-NMR experiments which showed that the bilayer to H_{II} transition of PE molecules is shifted to lower temperatures in the presence of BLM; a fracture of the PE organize themselves in H_{II} structures even below the gel to liquid-crystalline phase transition temperature of pure PE. Thus, these results demonstrated the ability of BLM to induce H_{II} in PE systems. The results of the effect of BLM on CF leakage from multilamellar PE vesicles are summarized in the table:

	Release (%)			
Internal medium	CF in buffer (pH 7.4)		CF in 1 M	BLM(pH 7.4)
External medium	t = 25°C	t = 44°C	t = 25°C	t = 44°C
Buffer	73.8	76.8	50.6	71.7
BLM	68.9	93.8	56.3	83.0
Internal medium	CF in buffer (pH 9.5)		CF in 1 M	BLM(pH 7.4)
External Medium	t = 25°C (pH 9.5)	t = 25°C (pH 7.4)	t = 25°C (pH 9.5)	t = 25°C (pH 7.4)
Buffer	51.3	75.7	45.9	78.1
BLM	50.0	93.7	36.5	88.2

Interaction of the lipid surface with BLM, resulted in a less permeable bilayer but also one more prone to H_{II}. Once the H_{II} is formed, all vesicle contents are lost. Thus, although BLM can profoundly stabilize liposomes, also can induce H_{II} formation resulting in the loss of vesicle contents.

Th-AM-E8

GENERATION OF A RE-ENTRANT HEXAGONAL(II) - LAMELLAR(α) - PHASE DIAGRAM FOR DOPE-WATER MIXTURES USING MEASURED HEATS OF TRANSITION AND WORKS OF HYDRATION

Klaus Gawrisch, V. Adrian Parsegian, NIH, Bethesda, MD
Damian A. Hajduk, Mark W. Tate, Sol M. Gruner, Princeton Univ, Princeton, NJ
Nola L. Fuller, R. Peter Rand, Brock Univ, St. Catharines, Ontario

We have examined the hexagonal - lamellar - hexagonal phase transition that occurs with the continuous dehydration of dioleoylphosphatidylethanolamine (DOPE) water dispersions. Using 31P, 2H NMR and X-ray diffraction in combination with osmotic stress, we have measured the free energy changes in both phases as a function of water concentration. Consistent with a low measured enthalpy of 0.3 kcal/mol and the temperature sensitivity, the hexagonal - lamellar transition requires little osmotic work -- only about 0.1 kT per DOPE molecule to go from full hydration to the point of transition at 22°C. Based on these data we have been able to recreate the double phase transition as a function of water concentration and temperature. The phase diagram so generated shows the experimentally observed re-entrant behavior of the phase transition and thus supports the use of osmotic stress measurements to derive free energies.

Th-AM-E9

DEUTERON NMR RELAXATION STUDIES OF PEPTIDE-LIPID INTERACTIONS -- Scott Prosser and James H. Davis, Dept. of Physics, University of Guelph, Guelph, Ontario, Canada, N1G 2W1; Christian Mayer, Klaus Weisz and Gerd Kothe, Inst. of Physical Chemistry, University of Stuttgart, Pfaffenwaldring 55, D-7000 Stuttgart 80, Germany

A unique model membrane system composed of a synthetic amphiphilic peptide (Lys_2-Gly-Leu_{16}-Lys_2-Ala-amide) and specifically labelled phospholipids (7,7-$^2H_2$-1,2-dipalmitoyl-sn-glycero-3-phosphocholine and 2,2-$^2H_2$-1,2-dipalmitoyl-sn-glycero-3-phosphocholine) has been studied by ^2H NMR. The structure and organization of the peptide in the bilayer, in addition to the phase boundaries of the fluid and gel phases, have been determined previously. The system was studied from -60°C to 60°C, at molar peptide concentrations of 0%, 2%, 4% and 6%, using inversion recovery, quadrupolar echo and in some cases Jeener-Broeckaert sequences. Analysis of the experiments, employing a density matrix treatment, based on the stochastic Liouville equation, revealed information about the dynamic organization of the lipid in the different membrane phases. This dynamic organization is described in terms of segmental and molecular order parameters and in terms of correlation times corresponding to both inter- and intramolecular motions, comprising overall reorientation of phospholipid molecules as a whole, trans-gauche isomerizations of individual chain segments, and collective order director fluctuations. The influence of the synthetic peptide on these parameters was thus determined.

Th-AM-E10

A GENERAL MODEL FOR THE INTERACTION OF DRUGS, ANAESTHETICS, AND INSECTICIDES WITH LIPID MEMBRANES

Kent Jørgensen,[1,2] John Hjort Ipsen,[2] Ole G. Mouritsen,[2] and Martin J. Zuckermann[3]

[1]The Royal Danish School of Pharmacy, DK-2100 Copenhagen Ø, Denmark; [2]The Technical University of Denmark, Building 307, DK-2800 Lyngby, Denmark; [3]McGill University, Montreal, PQ, H3A 2T8, Canada

A general microscopic interaction model is proposed to describe the changes in the physical properties of phospholipid bilayer membranes due to foreign molecules which, to different degrees, partition between the membrane phases and the aqueous environment. The model is a multi-state lattice model for the main phase transition of lipid bilayers and the foreign molecules are assumed to intercalate as interstitials in the lattice. By varying the model parameters, the diversity in the thermodynamic properties of the model are explored using computer-simulation techniques which faithfully take account of the thermal fluctuations. A classification of the diverse thermal behavior, specifically with regard to the phase diagram, the specific heat, the density flutuations, and the partition coefficient, is suggested with a view to rationalizing a large body of experimental measurements of the effects of different foreign molecules on membrane properties. The range of molecules includes diverse compounds such as volatile general anaesthetics like halothane, cocaine-derived local anaesthetics like procaine, calcium-channel blocking drugs like verapamil, antidepressants like chlorpromazine, and anti-cancer agents like adriamycin. A particular result of the work is the finding that anaesthetics and insecticides have a strong effect on the lateral heterogeneity of the membrane inducing regions of locally high concentration. This leads to a broadening of the specific heat and a maximum in the membrane/water partitioning coefficient, in agreement with experimental data.